Smart Structures and Systems, *Vol. 30, No. 6 (2022) 687-701*
https://doi.org/10.12989/sss.2022.30.6.687

Structural health monitoring response reconstruction based on UAGAN under structural condition variations with few-shot learning

Jun Li [2], Zhengyan He [1] and Gao Fan*[1]

[1] *School of Civil Engineering, Guangzhou University, Guangzhou 510006, China*
[2] *Centre for Infrastructure Monitoring and Protection, School of Civil and Mechanical Engineering, Curtin University, Bentley, WA 6102, Australia*

(*Received June 24, 2022, Revised October 6, 2022, Accepted November 3, 2022*)

Abstract. Inevitable response loss under complex operational conditions significantly affects the integrity and quality of measured data, leading the structural health monitoring (SHM) ineffective. To remedy the impact of data loss, a common way is to transfer the recorded response of available measure point to where the data loss occurred by establishing the response mapping from measured data. However, the current research has yet addressed the structural condition changes afterward and response mapping learning from a small sample. So, this paper proposes a novel data driven structural response reconstruction method based on a sophisticated designed generating adversarial network (UAGAN). Advanced deep learning techniques including U-shaped dense blocks, self-attention and a customized loss function are specialized and embedded in UAGAN to improve the universal and representative features extraction and generalized responses mapping establishment. In numerical validation, UAGAN efficiently and accurately captures the distinguished features of structural response from only 40 training samples of the intact structure. Besides, the established response mapping is universal, which effectively reconstructs responses of the structure suffered up to 10% random stiffness reduction or structural damage. In the experimental validation, UAGAN is trained with ambient response and applied to reconstruct response measured under earthquake. The reconstruction losses of response in the time and frequency domains reached 16% and 17%, that is better than the previous research, demonstrating the leading performance of the sophisticated designed network. In addition, the identified modal parameters from reconstructed and the corresponding true responses are highly consistent indicates that the proposed UAGAN is very potential to be applied to practical civil engineering.

Keywords: deep learning; few-shot learning; self-attention; structural health monitoring; structure response reconstruction

1. Introduction

With the ageing of civil infrastructures, structures will be inevitably damaged or degraded due to over loading, material degradation, extreme environment, etc., that may cause serious structural failure or even collapse. Therefore, the real-time SHM systems installed on civil infrastructures to continuously monitor the lifecycle structural conditions, are significant for engineers to timely detect structural damage and assess the operational condition to prevent hazards (Cross *et al*. 2013, Yi *et al*. 2013, Klikowicz *et al*. 2016, Nagarajaiah and Erazo 2016). Structural responses data collected by SHM system that contain important structural information are critical to determine the current structural condition. However, due to the incompleteness of measured structural information that is mainly limited by the budge of SHM systems, once any of the structural response data lost, it could be difficult to accurately determine the actual state of structures from the remaining incomplete data (Bao and Li 2021). Despite the reliability of the system hardware including sensors, transmission modules, data acquisition systems and data storage modules has been advanced constantly, data loss still occurs unexpected especially when SHM systems undergo long-term service or extreme loading (Kullaa 2013). SHM data loss is now a critical barrier to the development of SHM techniques. Therefore, it is in urgent demand to develop an effective approach that can timely and accurately reconstructs the lost response data.

Current researches on structural response reconstruction can be broadly divided into the finite element model (FEM) based methods and data driven methods (Sun *et al*. 2020). FEM based methods extract the response transmission function or correlation between system degrees-of-freedom (DOFs). The lost data can be predicted by transferring the available data to DOFs of lost data using the derived transmission function or correlation. Once a precise FEM is built for the target structure, responses can be reconstructed efficiently. On the other hand, data driven methods build a mathematical model to simulate the transmission function between measurement points. In contrast with FEM based methods, data driven methods mine the hidden abstractive features of structural responses and establish the instinctive mapping between measurement points from previously

*Corresponding author, Ph.D.,
E-mail: gao.fan@gzhu.edu.cn

ISSN: 1738-1584 (Print), 1738-1991 (Online)

measured complete data. The lost data can be predicted with the established model. The whole process of data driven methods is undertaken automatically with few engineering interventions.

Among the FEM based approaches, Li *et al*. (Li *et al*. 2013, Li and Hao 2014) and Law *et al*. (2011) used the transmissibility matrix derived from the frequency response function (FRF) or impulse response function to transform the vibration response data measured from other positions into desired positions. He *et al*. (2016) combined the transmissibility matrix with the empirical modal decomposition (EMD) technique to reconstruct the strain or stress responses at locations where the responses are poorly measured. The method decomposed the structural responses into several modal responses and reconstructed the stress-strain responses of critical DOFs using independent transfer equations of the intrinsic modal functions. Wan *et al*. (2014) developed EMD based method to improve the reconstruction of closely spaced modes and then extended this method to nonlinear damping systems. Kalman filter is a classic tool for response prediction (Petersen *et al*. 2018, Zhang and Wu 2019). It provides an unbiased and recursive algorithm to estimate the unknown state vector of a linear dynamic system using incomplete data set (Kalman 1960). Zhang and Xu (2016) proposed a Kalman filter-based multi-type responses reconstruction technique and combined it with response sensitivity for damage localization. Zhu *et al*. (2013) fused limited multi-type data and reconstructed the critical multi-scale structural responses by using Kalman filter. Zhang *et al*. (2021) used modal signal to noise ratio (MSNR) to select the modes that contribute significantly to the structural response. It subsequently reduces the data dimension and complexity in state estimation of civil structures by Kalman filter algorithm. Niu *et al*. (2015) used Kalman filter to simultaneously reconstruct the structural acceleration and wind load online. The FEM based methods for responses reconstruction require the FEM of target structure to be preciously established to obtain accurate transmission relationship between structural DOFs. However, the modelling errors due to unavoidable structural material uncertainties, structural damage, model simplification method, variation of environmental and operational condition (Ni *et al*. 2018, 2019b), and the coupling with the stochastic actions of the loads (Ni *et al*. 2019a) severely distort the quality of reconstructed data. The application of FEM based methods to practical engineering is still challenging.

The data driven methods, especially machine learning algorithms, have attracted significant attentions in structural response reconstruction. The previous studies have shown that the traditional machine learning based methods (Bao *et al*. 2013, Huang *et al*. 2014, Thadikemalla and Gandhi 2018) are available for response reconstruction, but the accuracy is unsatisfactory for practical structures that are large and complex. Recently, with the rapid development of computational power and machine learning algorithms, especially deep learning, the research of data driven structural response reconstruction is highly emphasized. Deep learning in processing SHM data has been widely investigated in response noise reduction (Fan *et al*. 2020), damage identification and localization (Lin *et al*. 2017) and sensor anomaly data detection (Zhang and Lei 2021), etc. Common networks used for structural response reconstruction can be classified as three groups, convolutional neural network (CNN) based, recurrent neural network (RNN) based and generative adversarial network (GAN) based networks. Among the utilized CNN networks, Oh *et al*. (2020) proposed a structural lost strain monitoring data recovery method based on two-dimensional CNN. The time series are rearranged as two-dimensional maps to adapt the network, while adding artifacts to input data. Li *et al*. (2022) proposed a multi-type full-field response reconstruction framework with autoencoder structure and skip-connected of CNN. Fan *et al*. (2019) firstly proposed a bottlenecked one-dimensional CNN for recovering random missing sampling points during wireless transmission. The reconstruction errors are acceptable until the loss ratio up to 80%. A densely connected neural network (DenseNet) was further developed and experimental studies were conducted with the acceleration responses of Guangzhou TV Tower to investigate the effect of measure points of input data, the number of available and unavailable measure points, and measurement noise (Fan *et al*. 2021a). For RNN, Jeong *et al*. (2019) proposed a bidirectional recurrent neural network (BRNN) for data reconstruction of a bridge. They calculated the covariance matrix between all sensors and selected the subset of sensors data with a high correlation to the response to be reconstructed. Jiang *et al*. (2021b) proposed a sequence to sequence model based on the bidirectional gated recurrent unit (BiGRU) and local soft attention (Luong *et al*.2015) for reconstructing dynamic responses and measuring information entropy error. Local soft attention focuses on the output of a single unit at a time, which improves local accuracy but inevitably loses important global features. In terms of the application of GAN, Lei *et al*. (2021) proposed a deep convolutional GAN in which the generators of the network have an encoder-decoder structure. The reconstructed acceleration data and strain data of a cable-stayed bridge model were used to identify the structural modes and vehicle loads of the bridge to show the effectiveness. Jiang *et al*. (2021a) used a GAN based unsupervised learning to impute missing strain response of single and multiple sensors based on the remaining intact data. Fan *et al*. (2021b) developed a segment based conditional GAN (SegGAN). The capability of the method was validated in feature extraction of structural response and response reconstruction of linear and nonlinear systems. The feasibility of using the reconstructed responses for damage detection was tentatively explored and proved effective.

It should be highlighted that among past studies, the target structures should be maintained a constant state in the mathematical model training phase and data reconstruction phase. If the structural condition changes with ageing or extreme loading condition, the mapping between measurement points alters consequently, leading the previous trained model invalid for reconstructing response in the altered structural state. Meanwhile, the ageing and extreme loading of structures are unfortunately corresponding to the fragile scenarios of SHM systems, which may be encountering long-term service and extreme

operational circumstances, causing the likelihood of data loss increased dramatically. To adapt the structural condition changes and improve the universality of data driven methods, the existing methods require a comprehensive training dataset containing a huge number of response samples that are measured under all possible working scenarios. However, it consumes a large amount of time and manpower to prepare a dataset representing the lifecycle structural conditions. Besides, complete structural response data in some states are very rare. Generating such a dataset is impractical for infrastructure. Therefore, it requires the model to be universal, which can learn the representative features and establish generalized mapping efficiently by using a small and imperfect training dataset.

The problem of mining features from limited data samples is also known as few-shot learning. In this case, the recent research hotpot GAN framework, that simultaneously trains a generator model and a discriminator model in an unsupervised manner to fully leverage the limited training samples, is adapted for addressing the response reconstruction under varying structural conditions. GAN framework (Goodfellow *et al*. 2020) facilitates the extraction of features from fewer samples and hence speeds up the convergence of network by playing mutual adversarial games between the generator and discriminator. It is also highlighted by its powerful capability on extracting detail features of data. As a result, GAN has been widely applied in pixel to pixel task, such as image generation (Bao *et al*. 2017), image text conversion (Xu *et al*. 2018) and style transfer (Zhang *et al*. 2017). Structural response reconstruction is also a sampling point to sampling point task, it is therefore promising to transfer the advantage of GAN to response reconstruction. Besides enhancing local detail feature mining, self-attention technique (Vaswani *et al*. 2017) is an efficient way to improve the efficiency of global feature extraction by enlarging the perceptual field restricted by convolutional kernel size. A self-attention module computes the autocorrelation of the input feature maps to determine the contribution of each element. The elements that are strongly correlated with others are weighted as the representative features. In this way, the instinctive temporal correlation of data is also excavated. Due to its excellent performance in extracting long-distance dependency and global features, there have been many applications of self-attention for time series prediction (Lin *et al*. 2020, Zhou *et al*. 2021).

In this paper, a novel approach based on U-shaped dense blocks and self-attention technique reinforced generative adversarial network (UAGAN) are proposed for structural response reconstruction under varying structure conditions with a few-shot learning manner. The specific network is sophisticatedly designed to facilitate the mining of representative and universal features from a small sample of datasets. Adversarial training framework, U-shaped dense blocks and self-attention modules are employed to fully use the temporal and spatial correlation between responses for reconstruction. The loss function to tune network parameters is also carefully designed considering the particular requirement for SHM. To elaborately describe the proposed method and the validation of the effectiveness and robustness on response reconstruction under varying structural conditions with a small number of sample datasets, the following contents are arranged as follows. Section 2 firstly explains the theoretical development of UAGAN for response reconstruction. The architecture of the network is described from overall structure to specific modules, including their detailed configurations, functions and characteristics. Section 3 presents a numerical study using simulated data of a seven-layer steel frame model under normal, random material degradation and structural damage states. The performance of the proposed UAGAN is compared with an advanced CNN model to investigate the feature of UAGAN and demonstrate the significance of employing adversarial training framework and self-attention module. Section 4 presents an experimental study with a frame structure to validate the applicability of UAGAN to practical structures. The structural responses measured under ambient excitations and earthquake excitations are processed as training and testing datasets to verify the effectiveness and robustness of this network in addressing the effect of changes in structural environmental and operational conditions. Frequency domain decomposition (FDD) method is used for modal parameters identification of the actual response and the reconstructed response, to evaluate the performance of reconstructing structural characteristics. Section 5 summarizes the results and findings of this study.

2. Methodology

The proposed UAGAN is a specific GAN that features self-attention module and U-shaped dense blocks. UAGAN inherits the adversarial training framework which fully utilizes the advantage of GAN for few-shot learning. UAGAN replaces the layer-to-layer connected convolutional layers in the generator by successive U-shaped dense blocks to improve the information flow among the network, which consequently raises the efficiency of feature extraction and mitigates the overfitting effect. For a single U-shaped dense block, it performs as a mini U-Net (Ronneberger *et al*. 2015) that efficiently extracts the higher-level features while filtering noise components during down sampling and up sampling of data. Self-attention module is embedded in the generator after dense blocks to emphasis the long-distance intrinsic correlations and weight the important features. The designed loss functions compute the error of reconstructed responses in the time and frequency domains, in view of the application for SHM. Combining the adversarial training framework with U-shaped dense blocks and self-attention module can greatly facilitate UAGAN to extract more representative global and local features from a small sample dataset, leading UAGAN adaptable to complete the response reconstruction under varying structural conditions in a few-shot learning manner.

2.1 The architecture of UAGAN

The underlying architecture of UAGAN is GAN that is developed by Goodfellow *et al*. (2020) as a novel probabilistic generative model. The purpose of GAN is to

find out the statistical patterns within a given observed data and to sample completely new and similar data to the observed data based on the learned probability distribution. Before GAN, the parameters of generative networks are updated according to the loss functions defined by the engineers, which is totally based on the prior knowledge of data. In contrast, GAN introduce a trainable discriminative model to determine the probability of generated samples that are sampled from real data distribution, as shown in Fig. 1. Consequently, the purpose of the generative model is altered to learn more robust patterns from training datasets to better describe the real data distribution, thus to fool the discriminative model and to minimize the discriminative accuracy. While the discriminative model tries to maximize its accuracy by learning more representative features of real and generated data to clearly distinguish them. The optimization process of GAN is to find a Nash equilibrium between the generative and discriminant models. Through the continuous confrontation between these two internal models, the performance of generative model to describe the real data distribution, especially the details of real data are greatly improved.

The proposed network for response reconstruction is trained in a supervised manner. The training dataset consisted of paired input and label is prepared based on a period of complete data, stably measured by all the sensors of SHM systems. The input is selected as the response of sensors that constantly operate normally. For response reconstruction, the output of models should be the response of sensors with data loss occurred after a period of normal recorded. Therefore, the label of training samples is the actual measured response of the fault sensors that is recorded at the same time period with the input. It should be noted that even this network is called supervised training, the label of input can be generated automatically which saves a lot of time and manpower on labeling work. In UAGAN, the generator is proposed to represent the mapping between the input and label, and the discriminator is used to facilitate the generator to learn more representative and universal features. Therefore, the input

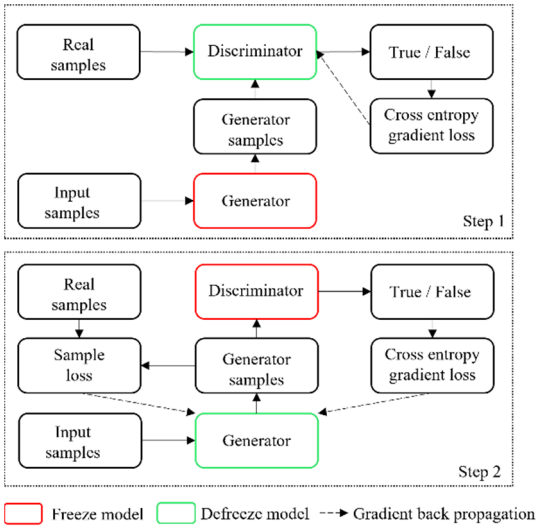

Fig. 1 Schematic diagram of adversarial training framework

of the generator is the available response of constantly well-functioning sensors and the output is the response from later faulty sensors, which are measured in the same time. The generator reconstructs responses, and the corresponding real response are grouped as the input of the discriminator. The discriminator is a layer-to-layer CNN to gradually refine the higher-level abstractive features and later establish the mapping between extracted features and label. To allow the discriminator distinguish the generated and real responses, the label for the input is automatically defined, where 1 means 'true' which is given to real data and 0 denotes 'fake' which is allocated to generated data. Defining such labels for input samples promotes the discriminator to extract more distinguished features and judge the source of real and generated data. For example, when the discriminator confuses with a generated sample and offers a predicted value close to 1, the discrepancy between label and prediction becomes large and a subsequently great gradient will be produced to tune model parameters violently.

2.2 The generator of UAGAN

Determining the capacity of a network model to a specific dataset is challenging. A shallow network such as artificial neural network (ANN), tends to be incapable of extracting representative features of data and failing to establish the mapping between network input and output. On the other hand, a deep network with complex structure and larger capacity is more functional for engineering problems. However, deep networks may result in the reduction of model generalization, which is known as overfitting. For structural response reconstruction, the training data are mainly composed of structural vibration information and measurement noise. Both components are varying with time and environmental and operational conditions. There are high demands on the generator to accurately capture the universal and representative features of data, while minimizing the effect of noise. To ensure the effectiveness of applying UAGAN for reconstructing the structural responses under various structural states, the generator is sophisticatedly designed as a two-way parallel structure. The structure of the generator is simple but all the used modules are highly professional in their particular tasks. The main feature extraction sequence consists of three dense blocks and one self-attention module as shown in Fig. 2. It is a classic structure composed of the most advanced deep learning modules to gradually refine the features with a high level of abstraction. In a U-shaped dense block, the compression layers halve the size of feature maps to remain the key robust features in a higher dimension. This process also effectively eliminates the noise components without any constant patterns. The results of the dense blocks are connected via skip-connection to boost the information flow and consequently improve the generalization capability for few-shot learning. The extracted features of each dense block are fused as the input of the self-attention module. The auxiliary sequence starts with the feature extraction by a dense block and feature maps resizing by a followed convolutional layer. To mitigate overfitting when training by simple data with fewer features, the assistant sequence before fully connection

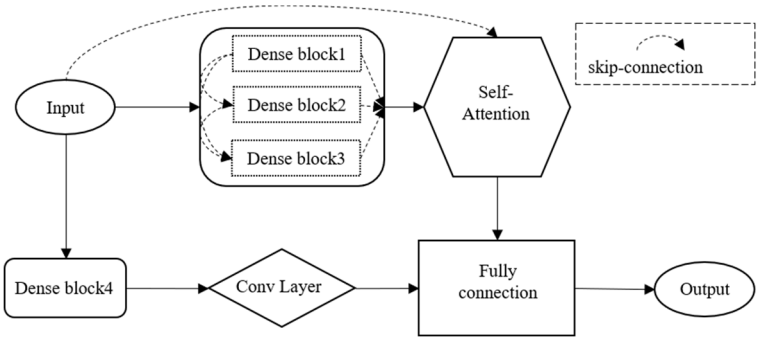

Fig. 2 The structure of the generator

Table 1 The detail configurations of the generator

Layer	Kernel number	Kernel size	Input shape	Output shape	Activate
Dense block 1	256	16	(1024,6)	(1024,256)	Leaky ReLU
Dense block 2	128	32	(1024,262)	(1024,128)	Leaky ReLU
Dense block 3	64	64	(1024,390)	(1024,64)	Leaky ReLU
Self-Attention			(1024,454)	(1024,1)	
Dense block 4	64	64	(1024,6)	(1024,64)	Leaky ReLU
Conv layer	1	2	(1024,64)	(1024,1)	Leaky ReLU
Fully connection layer			(1024,2)	(1024,1)	Leaky ReLU

layer is pre-trained based on datasets to bridge the input and output in a shorter way. This sequence also offers supplementary low-dimensional features that may lost during successive convolution to the main sequence. These low and high-dimensional features are fused as comprehensive feature maps and subsequently used as input to a fully connection layer to predict output response. The fully connection layer has the same length of input samples, and is only one convolutional kernel to finally resize the features complying with the output size. The initial network setting of the hyperparameters and configurations are designed based on the previous experiences and then tuned by trial and error. The optimal settings, such as filter number, kernel size, number of layers and learning rate, etc., are finally determined as the configuration that has the smallest validation loss. The hyperparameter configurations of the generator are shown in Table 1.

2.2.1 U-shaped dense block

The U-shaped dense block has a bottlenecked structure consisted of two channel reduction layers, one bottleneck layer and two channel increasing layers as shown in Fig. 3. Larger convolutional kernels allow the increased perceptual field to extract the features of approximate fuzzy of data. In contrast, smaller convolution kernels are specialized for extracting microscopic and detail features of the data such as peaks and rapid changes. The proposed U-shaped dense block which consists of both larger and smaller convolutional kernels, is more effective to learn comprehensive features. A U-shaped dense block has a feedforward feature flow which compresses features and then gradually expands to their original channels by a factor of 0.5. The input data are firstly processed by the reduction layers and bottleneck layer to extract high-dimensional and robust features. Meanwhile, the measurement noise components without any certain pattern are filtered by the compression operation. However, response features will inevitably be lost during multiple layer-to-layer convolutional computation, especially for feature compression. To ensure that important features are properly delivered to the following layers, densely skip connections are applied to link the extracted features of each convolutional layer to all subsequent layers within a dense block, and also pass the features of preceding dense blocks to following dense blocks as shown in Fig. 3. Skip connections deliver low-dimensional features to deeper layers directly, allowing the gradients shuttle between layers and modules to prevent gradient explosion or vanishing.

A U-shaped network generally consists of a feature compression path and a feature expansion path. Among the computational flow of compression path, UAGAN as a U-shaped network, extracts the vibration features of the response through the successive convolutional layers (Lin *et al*. 2017). The down-sampling part of the U-shaped

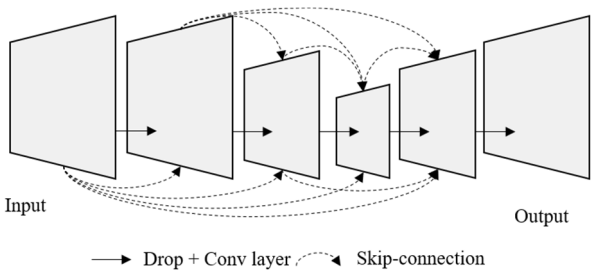

Fig. 3 The structure of a U-shaped dese block

network discards unstable features when compressing and extracting high-dimensional features, which indeed sifts the noise components (Fan *et al*. 2020). The up-sampling path expands the size of feature maps to improve the resolution of features. Attributing to the symmetrical structure of U-shaped network, the layers at the mirror position contain a large number of features with the same level of abstraction, which are further fused by skip-connection to enrich the features for reconstructing data and prevent the loss of important information.

2.2.2 Self-attention module

The original self-attention technique was introduced in (Vaswani *et al*. 2017) to facilitate the establishment of correlation between multiple modal inputs in the sequence-to-sequence task. It is remarkable that the features extracted from structural responses by CNN-based models can be explained as the structural vibration characteristics from the perspective of engineers, as proved in Ref. (Lin *et al*. 2017, Fan *et al*. 2021a). However, a period of input structural responses from multiple measurement points, in fact include both spatial correlations among measurement points and temporal correlations between sampling points measured at different time steps. Therefore, it is crucial to utilize the entire information of responses to build a more effective mapping between input and output responses. The original self-attention that only computes the channel-wised correlation among input responses cannot completely utilize the response data features. To facilitate response reconstruction, the original self-attention channel-wise attention is modified to element-wised attention, which focuses on the correlation between every two feature elements to capture the long and short dependency between elements. Then, the output of the self-attention module is attentive feature maps, generated by weighting the sum of input elements based on the attention score. The calculation process of attention mechanisms can be expressed as follows.

$$Attention(Q,K,V) = \text{Linear}\left(SoftMax\left(\frac{QK^T}{\sqrt{d_k}}\right)V\right) \quad (1)$$

The input data initially pass through three individual fully connected layers to obtain three transfer matrices named Query (Q), Key (K), and Value (V). This process is equivalent to a transformation of the input, which can improve the fitting ability of the network. The preliminary attention score is computed by the transpose dot product of Q and K matrices. Due to the large variance of the distribution in the matrix, the gradient of some elements in the attention score matrix is too small. The preliminary attention score matrix is then normalized by the square root of the k-matrix dimension $\sqrt{d_k}$, and finally transferred to a probability value by SoftMax. The weighted output is computed as the multiplication of normalized attention score matrix and value matrix V. For CNN-based networks, the expansion of the perceptual field is realized by consistent down sampling of feature maps. However, the volume of network parameters and the lost features increase dramatically with the depth of the network. For few-shot learning, a small sample of data provide insufficient information for training networks. The model parameters frequently fall into local optimal solutions, leading to the reduction of generalization. In contrast, the modified self-attention module optimizes the globality of features extracted by dense blocks to offer more universal and representative features for response reconstruction.

2.3 The discriminator of UAGAN

The discriminator of UAGAN is a fully CNN. The input of the discriminator is the concatenation of generated and the corresponding true structural responses, and the output is logical judgment values of 0 to 1 indicating the possibility of input samples that are from the true dataset. For structural response reconstruction, the discriminator facilitates the generator to build a more distinguished mapping between input and output responses by continuously providing gradients to tune the model parameters of the generator. From another perspective, the discriminator is a self-updated loss function that is progressive with the training process. The structure of the discriminator consists of three continuous convolutional blocks with a decreasing number and size of convolutional kernels. Each convolutional block in turn consists of three convolutional layers with amplified kernel size, as detailed in Fig. 4. The whole structure is gradually shrinking to compress features, while the individual block expanses feature within the block. In the discriminator, the extracted feature maps continuously shrink to be more sensitive to subtle changes in the responses. The convolutional layers in convolutional blocks are continuously enlarged, that in turn provide wider fields of sensation. This special up-down sampling network design can facilitate the discriminator to extract comprehensive and representative features. As a result, a delicate mapping between input responses and the output logical value can be established accordingly.

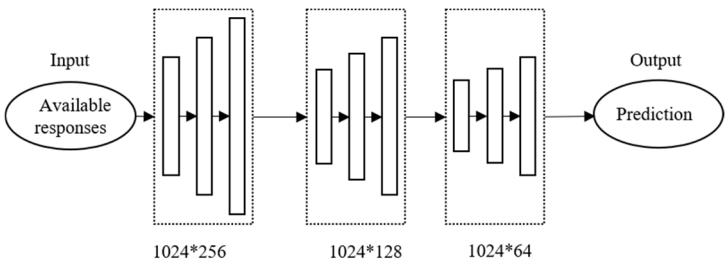

Fig. 4 The structure of the proposed discriminator

2.4 Loss function

A network measures the error between the predicted results and corresponding labels to produce a gradient for tuning model parameters based on the designed loss function. By minimizing the loss and adjusting the model parameters by a back-propagation algorithm, the network is gradually optimized and the prediction keeps approximating the label. The loss function of a network needs to be carefully designed to adapt to specific tasks. For structural response reconstruction, the target is to allow the network to learn correct mapping between responses of constantly available and later sensor fault measurement points by supervised training. Therefore, the target of the loss function is to minimize the discrepancy between reconstructed responses and labels. The original GAN applied to data generation has only one loss function to compute the error between the predicted logical value by discriminator and the corresponding label. However, the required accuracy for structural response reconstruction is point-wised for reliable structural condition assessment. A loss function of the discriminator that only determines the 'truth' of the entire input response is unable to meet the requirement. To facilitate UAGAN to learn both low-structure and high-structure features of data, the loss function of UAGAN is defined as two parts: an additional second norm (L2) sense function of the generator and a logical loss function of the discriminator.

The loss function of the discriminator is a cross-entropy function, which is the common loss function of GAN. It is expected that the discriminator always judges the response generated by the generator as fake, i.e., the prediction of discriminator tends to be 0. Meanwhile, the real data samples are always judged as true and the predictions are close to 1. As a result, the loss function of the discriminator is given in the following equation

$$D_{loss} = E\big(D(x)\big) + E\left(1 - D\big(G(z)\big)\right) \tag{2}$$

$$E(x) = -ones(x) \times \sum log\, x \tag{3}$$

where E denotes the cross-entropy calculation. In Eq. (3), $one(x)$ is an array consisting of 1 with the same shape as x, $D(x)$ and $D(z)$ are the predictions of the actual data sample x and generated sample z, respectively.

The loss function of generator consists of three components: time domain averaged L2 parametric loss, frequency domain averaged L2 parametric loss and logical loss offered by the discriminator. By combining L2 losses of data in the time and frequency domains, the network is promoted to accurately reconstruct wave forms and amplitudes of response, meanwhile, guarantee the consistency of instinct natural frequencies with the target structure. By applying the combined loss function of the generator, the effectiveness and usability of the reconstructed response for subsequent structural assessment and modal identification can be greatly optimized. The loss function of the generator is formulized as

$$G_{loss} = \frac{1}{N}\frac{\sqrt{\sum_{i=1}^{N}(y_i - x_i)^2}}{\sqrt{\sum_{i=1}^{N}(y_i)^2}} + \frac{1}{N}\frac{\sqrt{\sum_{i=1}^{N}\big(fft(y_i) - fft(x_i)\big)^2}}{\sqrt{\sum_{i=1}^{N}\big(fft(y_i)\big)^2}} + E[\,1 - D(G(z))] \tag{4}$$

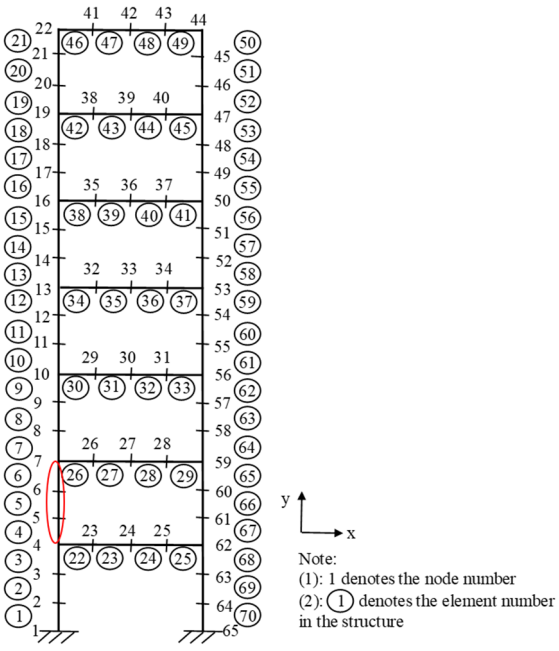

Fig. 5 FEM of the steel frame structure

where N is the number of samples in each batch, y_i and x_i are the ith elements of actual and reconstructed responses. *fft* denotes the Fast Fourier Transform operation. As shown in Eq. (4), the average L2 parametric loss used in this study is a normalized L2 loss that can provide stable gradient for generator. Compared with the common loss function for pixel-to-pixel tasks, the customized loss function involves the point-wised accuracy of responses in time and frequency domains and also the truth of data offered by a self-learned loss function. It is advanced in mining the real data distribution in a high-dimensional space.

Under the adversarial training framework, the generator and discriminator are trained alternatively. The discriminator is firstly tuned to ascend the gradients by enlarging the first and second terms of Eq. (2). Alternatively, the generator descends the gradient by tuning its parameters based on Eq. (4) and consequently minimize the gradient of the discriminator. After iterative training to complete the minimax competition, both the generator and discriminator enforce each other to learn distinguished features of structural response and facilitate the generator for establishing a generalized and robust mapping between input and output responses.

3. Numerical studies

To verify the effectiveness of the proposed method for reconstructing structural response under structural condition changes and a small number of sample datasets, numerical studies on a FEM of a seven-story steel frame is conducted. The FEM as shown in Fig. 5, is built based on an experimental even-story steel frame structure. The steel frame structure has a width of 0.5 m and a height of 0.3 m per floor, for a total model height of 2.1 m. The column and beam unit materials have a mass density of 7850 kg/m^3, a modulus of elasticity of 210 GPa, and cross-sectional dimensions of 50 mm × 5 mm and 50 mm × 9 mm, respectively. A concentrated mass is simulated by adding a 4 kg mass at the quarter and three-quarter positions of each floor to the corresponding vertical DOFs of the floors. The FEM is built using planar beam element, and each node in the FEM has three DOFs, that are translational displacements in the x and y directions and rotational displacement in the x-y plane, respectively. Each element of the FEM is defined as 0.1 m long, and the FEM of the frame model is hence meshed as 70 plane elements and 65 nodes. The model has a total of 195 system DOFs. The two fixed supports at node 1 and node 65 are modeled by constraining the corresponding DOFs at the bottom of the model. A sensitivity-based model updating method is used to determine the damping ratios of the frame structure (Li *et al*. 2017), and the damping ratios of the first two orders are calculated as 1.1% and 0.4%, respectively. The damping matrix is modeled by using Rayleigh damping. The initial finite element stiffness matrix and boundary conditions are updated based on the measured response of the experimental structure (Li *et al*. 2012). The updated model is used to generate structural responses by Newmark-beta method to prepare the training, validation and test datasets. The numerical studies under two practical scenarios, including random stiffness reduction and structural damage conditions are conducted to investigate the effectiveness and robustness of the proposed method under structural condition changes. The effect of measurement noise which is a serious adverse factor for data driven methods is also studied. In addition, the reconstruction results are compared with the results of a CNN with the same depth of UAGAN to investigate the improvement of using UAGAN for response reconstruction.

3.1 Random structural stiffness reduction

Structural stiffness reduction of civil structures is a common way of structural condition variation caused by inevitable material degradation under operational environment. The stiffness reduction consequently changes the structural vibration characteristics and behaviors, leading the extracted transmission function by FEM based methods less robust and data driven methods invalid under the changed state. A method to improve the capability of model in this situation is to collect the recent acceleration response for re-training, which is very time-consuming and impractical. Therefore, it is important to investigate the capability of UAGAN to learn universal and representative features from few samples and then reconstruct data with random structural stiffness condition changes occurred. To simulate such scenario, UAGAN is trained by using a short period of response measured under an initial structural condition without any stiffness changes. The lost response after random structural stiffness reduction occurred is reconstructed directly based on the trained UAGAN that never see any data under the new state.

400 seconds x-direction acceleration response from each floor of the frame model subjected to the ambient excitations are generated to prepare the training dataset. It is worth noting that 400 seconds of response as training data are extremely limited and critical for deep learning to refine representative features of data. The responses of nodes 4, 10, 13, 16, 19 and 21 are selected as available responses and node 7 is assumed as unavailable where the data loss is occurred after structural condition is changed. The random structural stiffness reduction is simulated by randomly reducing the elastic modulus of specific elements. To simulate the reduced stiffness, a normally distributed random stiffness reduction is assigned to each element of the FEM. The level of stiffness reduction ranges from 0% to 10%, where 10% random stiffness reduction causes significant variation in the vibration characteristics. The equation of simulating stiffness reduction can be expressed as

$$k_i' = (1 - SR) \times k_i \tag{5}$$

where k_i' is the reduced stiffness of the ith element, and SR denotes the stiffness reduction in this specific element.

The reduction of stiffness follows a standard normal distribution with the intensities of 1%, 2.5%, 7.5% and 10%. A comparison of the time series and the corresponding Fourier spectra for the original FEM and the FEM with modeling errors is shown in Fig. 6. 400 seconds response data with increasing stiffness reduction intensity are collected for validation and testing. 50% of the simulated response data of the model under 1% stiffness reductions are used for validation, and all the remaining data are processed for testing. The sampling rate is down sampled from 2000 Hz to 100 Hz, and the data are then scaled between -1 and 1. The training data is divided as 40 samples in terms of a sample length of 1024 points with overlap. The validation and testing datasets are divided as 20 samples with a length of 1024 points without overlapping. UAGAN and CNN are trained afterwards based on the minimal training samples. The training processes of UAGAN and CNN that are demonstrated by the training and validation losses are shown in Fig. 7. It can be seen from this figure, UAGAN converges rapidly and stably, indicating the strong performance on extracting the representative features and establishing mapping from a small number of sample datasets. The network is properly optimized with a minor validation loss around 0.04 after 200 training epochs. By comparing Fig. 7 (a) with (b), the final validation loss of UAGAN is much smaller than CNN with fewer training epochs. The results demonstrate that both the training efficiency and accuracy of UAGAN are better than CNN.

To explore the generalization capability of UAGAN, the

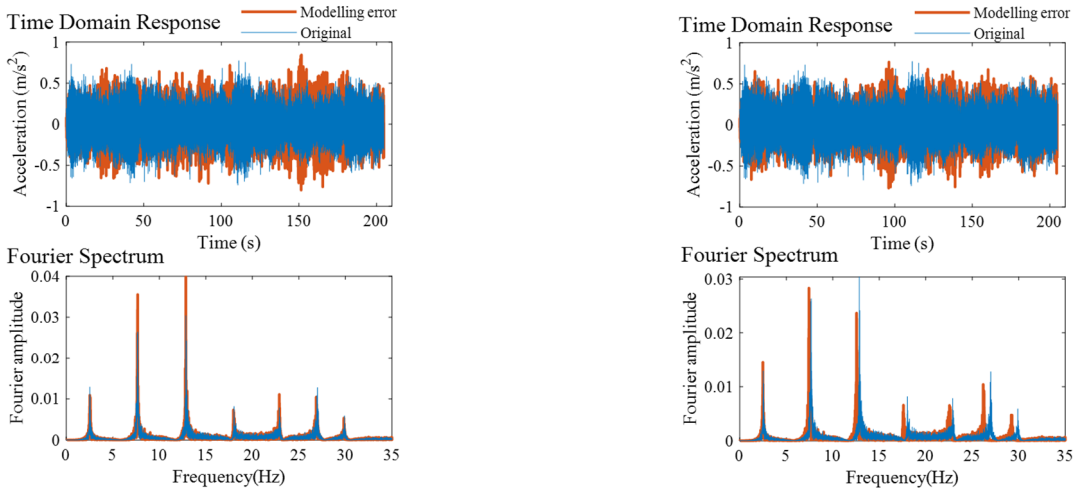

Fig. 6 Comparison of the responses for the original FEM and the FEM with modeling errors of (a) 1% and (b) 10%

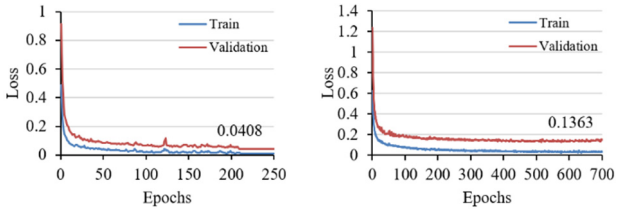

Fig. 7 The training losses of different network models with 1% modeling error: (a) UAGAN and (b) CNN

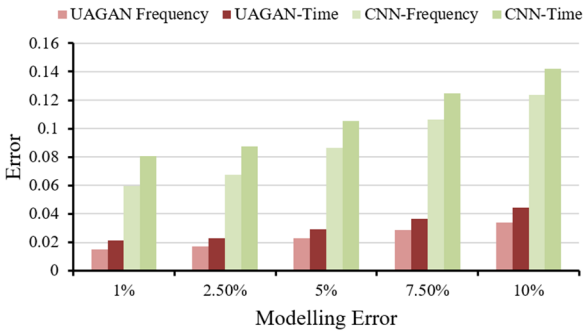

Fig. 8 Response reconstruction errors under 1%-10% modelling errors

lost acceleration data under 2.5%, 5%, 7.5% and 10% random stiffness reduction conditions are reconstructed using the trained UAGAN. The normalized reconstruction error that represents the error in a proportional form is calculated as

$$Error = \frac{\sqrt{\sum_{i=1}^{N}(y_i - x_i)^2}}{\sqrt{\sum_{i=1}^{N} y_i^2}} \tag{6}$$

where y_i and x_i are the ith sampling points of actual and reconstructed responses, respectively. The reconstruction errors under 1% to 10% stiffness reduction conditions are shown in Fig. 8. In this figure, it is remarkable that there is only about 2% rise in the reconstruction error of UAGAN along with the reduction intensity increasing from 1% to 10%. The reconstruction error is smaller than 4% despite that the structure stiffness is randomly changed for about 10%. The reconstructed response by CNN has larger errors compared with the actual responses, which may cause failure of structural condition assessment. Fig. 9 illustrates the reconstructed and actual responses under 10% random stiffness reduction condition. As shown in Fig. 9, the reconstructed responses by UAGAN show a high level of agreement with the actual responses in both time and frequency domains. In contrast, the reconstructed responses of CNN represent relatively large errors in the Fourier spectrum at the peaks of natural frequencies locations as marked in Fig. 9(b). The discrepancy of amplitudes will result in the errors in determining the vibration mode shapes. The results demonstrate that even if the structural condition changes significantly, the sophisticatedly designed UAGAN featured with dense blocks and self-attention module, effectively extracts universal and representative features from training samples to dynamically optimize the network with an outstanding generalization performance.

It should be noted that convolutional kernels also named as convolutional filters, function as self-learned band-pass filters when processing structural responses (Lin *et al.* 2017). In this way, the mined representative features from the acceleration responses are highly possible to be the vibration characteristics of the target structure. To further investigate the features learned by UAGAN, the middle-layer feature visualized technique is applied to the middle-layer training. It is widely accepted that the features extracted by shallow layers of deep neural networks are commonly easy to be understood by human being, therefore the output feature maps of the first dense block are isolated and visualized. The extracted feature maps are transferred to frequency domain by Fast Fourier Transform and the Fourier spectra of four representative feature maps are

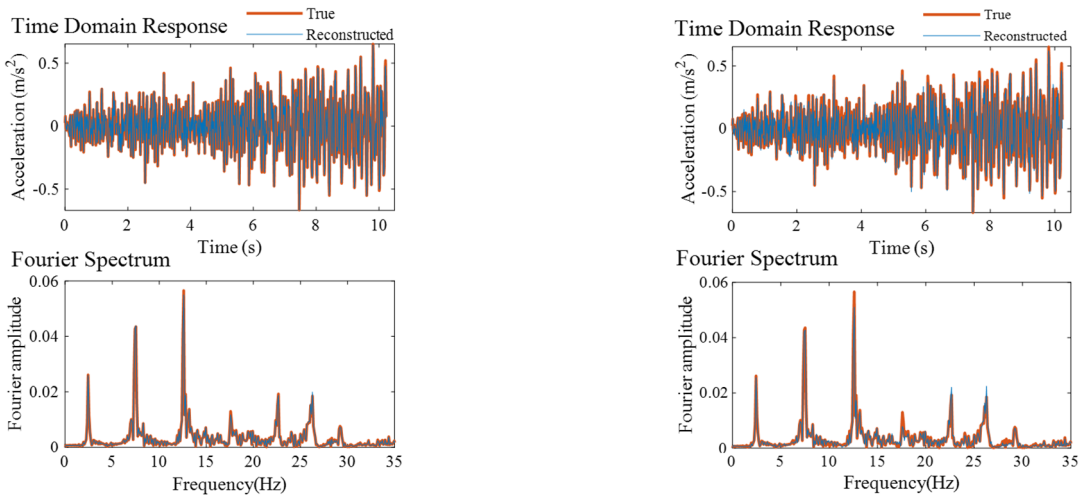

Fig. 9 Comparison of the reconstructed and actual responses under 10% random stiffness reduction condition by using: (a) UAGAN and (b) CNN

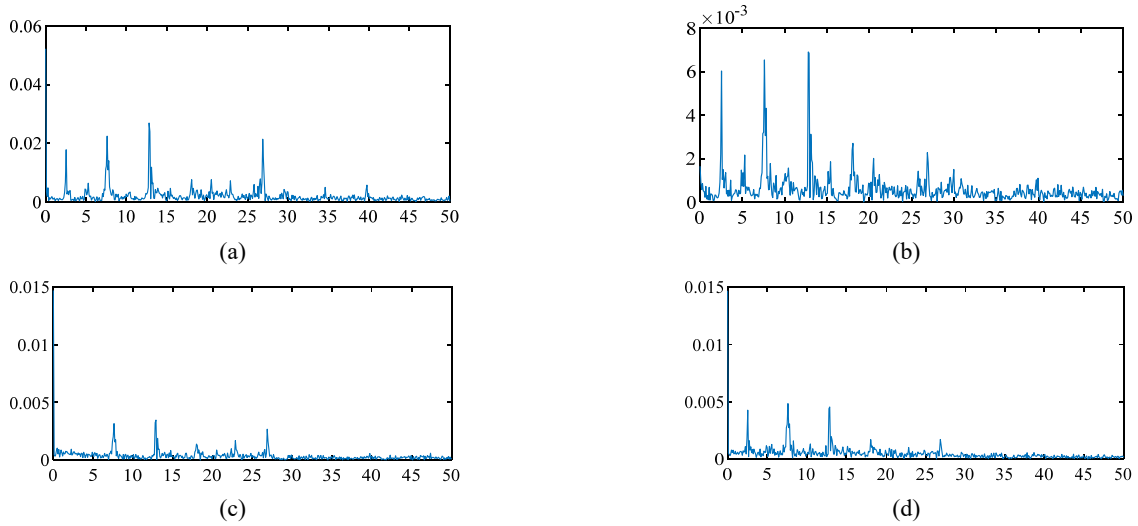

Fig. 10 Fourier spectra of the output feature maps of the first dense block

shown in Fig. 10. It can be observed that the peaks of the spectra are corresponded to the frequency bands of the structural frequencies, especially in first few modes. Dense block emphasized features can be explained as vibration modes of the frame structure from engineering aspect. The results coincident with the findings stated by Lin *et al.* (2017), which testifies that UAGAN has a strong capability on excavating meaningful features from acceleration responses.

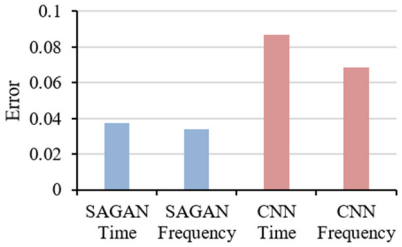

Fig. 11 Comparison of reconstruction errors with 20% stiffness damage

3.2 Reconstruction under structural damage state

Structural damage may suddenly occur without any alarm. Timely and accurately detect structural damage is significant for SHM, but is very dependent on complete and quality monitoring data. To involve structural damage in the FEM, the damage is simulated as a 20% stiffness reduction at the column of the second layer as marked in Fig. 5. 400 seconds responses of damaged structure are simulated and processed as the test dataset. Same experimental setup is applied and the above trained UAGAN and CNN models are used to reconstruct lost response after damage. As the local damage has a small effect to the entire structural behavior compared with random stiffness reductions, a minor variation in the vibration characteristics is caused. As a result, both networks show a very good capacity on

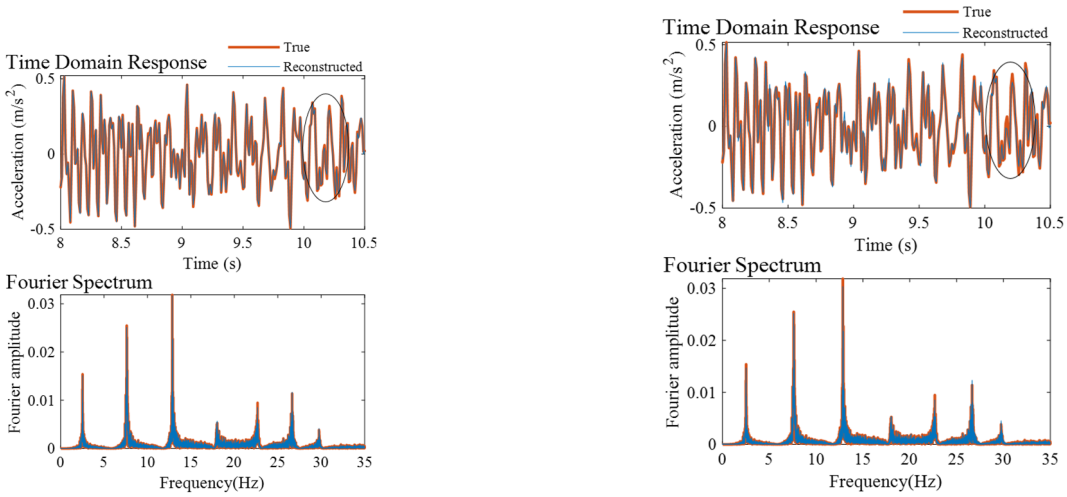

Fig. 12 Comparison of response reconstruction results with 20% stiffness damage by using: (a) UAGAN; and (b) CNN

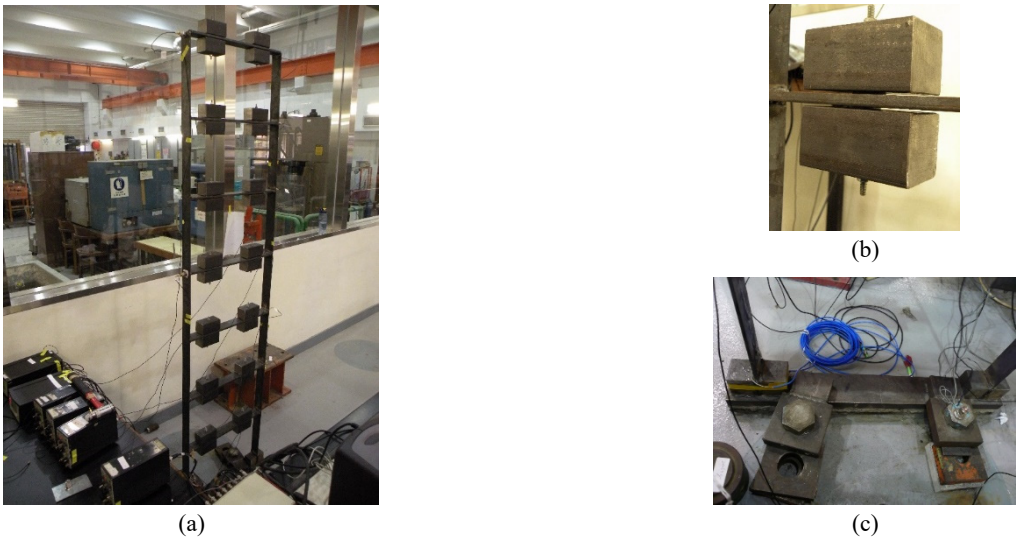

Fig. 13 Experimental seven-story frame structure: (a) Frame structure; (b) Mass blocks; and (c) Fixed supports

reconstructing response under structural damage, the errors are reduced by about 6% in the time domain and 3% in the frequency domain, as shown in Fig. 11. As circled in Fig. 12, UAGAN reconstructs better the details of responses in time domain, which demonstrates the superiority of dense blocks and self-attention module in feature extraction.

4. Experimental studies

The above numerical studies show that UAGAN is capable of reconstructing structural responses with structural state changes, including random stiffness reductions and structural damage. To investigate the applicability of UAGAN on field structures under varying operational conditions, the structural responses of the experimental seven-storey frame structure are used. The acceleration responses of the structure under varying operational and environmental condition and unmeasurable measurement noise are collected for training the UAGAN. The trained UAGAN model is later applied to predict the lost structural acceleration response under earthquake excitations. Modal parameters identification of the experimental frame by using the actual and reconstructed response is conducted to examine the capability of UAGAN to recover important information merged with the structural response and validate the applicability of the reconstructed responses for SHM.

4.1 Structural response reconstruction under earthquake excitations

Ambient and shake table tests are conducted for the above structure. It should be noted that ambient excitation sources include the surrounding operational machines in the laboratory and passing pedestrians. In the experimental tests, totally 7 sensors are mounted at one side of the column. The locations of sensors are at beam-column joint

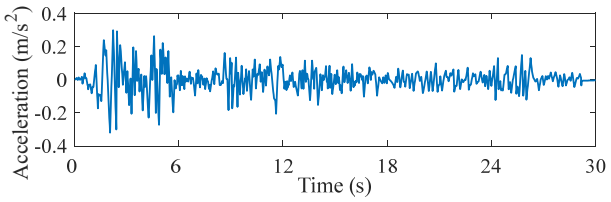

Fig. 14 Acceleration of El Centro earthquake

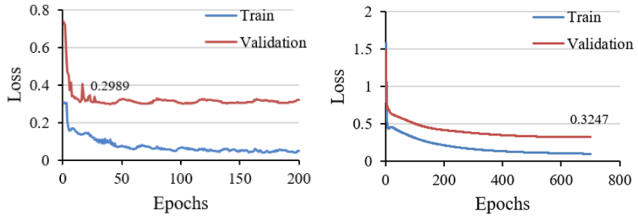

Fig. 15 Training processes of: (a) UAGAN (b) CNN

of each floor of the steel frame, as shown in Fig. 13. The top sensor is assumed to be faulty and responses of the rest of sensors are used as available responses. 14 minutes measured ambient responses are processed as training datasets followed the same procedure as introduced in the numerical studies. The trained network predicts the structural acceleration response under the recorded acceleration of El Centro earthquake as shown in Fig. 14. Consequently, with the limited measured ambient vibration responses, only 128 training samples and 32 validation samples with a length of 1024 are produced. The volume of training dataset is adaptable for few-shot learning.

The training processes of UAGAN and CNN are shown in Fig. 15 to demonstrate the convergence of two networks. The optimization process of UAGAN has a minor perturbation but finally dropped to a condition with a 0.025 smaller loss value than CNN. The comparison of the reconstructed and real responses in the time and frequency domains is shown in Fig. 16. In this case, with less nonlinearity of this steel frame under earthquake excitation, i.e., small structural condition change involved in the test, the reconstructed responses of both networks show a remarkable consistency with the ground truth with small reconstruction errors, namely, 16% and 17%. When carefully observing Fig. 16, it can be found that the details reconstructed by UAGAN are more perfect than CNN. However, compare with the previous work with the same experimental setup (Fan *et al*. 2021b), the employment of frequency domain L2 averaging loss significantly improves the low-frequency data structure extraction, that are natural frequencies and mode shapes of the structure. The experimental results demonstrate the effectiveness of the proposed method with few-shot learning for response reconstruction under minor structural condition changes but significant different excitations.

4.2 Modal identification using the reconstructed responses

The purpose of reconstructing the responses for SHM is to monitor the structural condition changes by analyzing the vibration characteristics. Typical modal parameters, such as natural frequencies and mode shapes, that reflect the vibration characteristics of the structure, are used for validating the applicability of the proposed network in practical engineering applications. Frequency domain decomposition (FDD) method is used to identify the modal parameters from the reconstructed responses and the corresponding actual responses measured under earthquake excitations. The identification results of the main modes of the frame are summarized and compared as shown in Table 2. The reconstructed responses contain totally the same components of vibration frequencies as the actual responses. The coordinate modal assurance criterion (COMAC) reaches to 99.96%, indicating that UAGAN effectively learns the universal and representative features of data from a small number of sample datasets. This finding is confirmed by the plot of the first order singular values of reconstructed and actual responses in frequency domain, as shown in Fig. 17. Both spectra are almost overlapped and the first six modes can be clearly detected, indicating that the proposed method can learn universal and

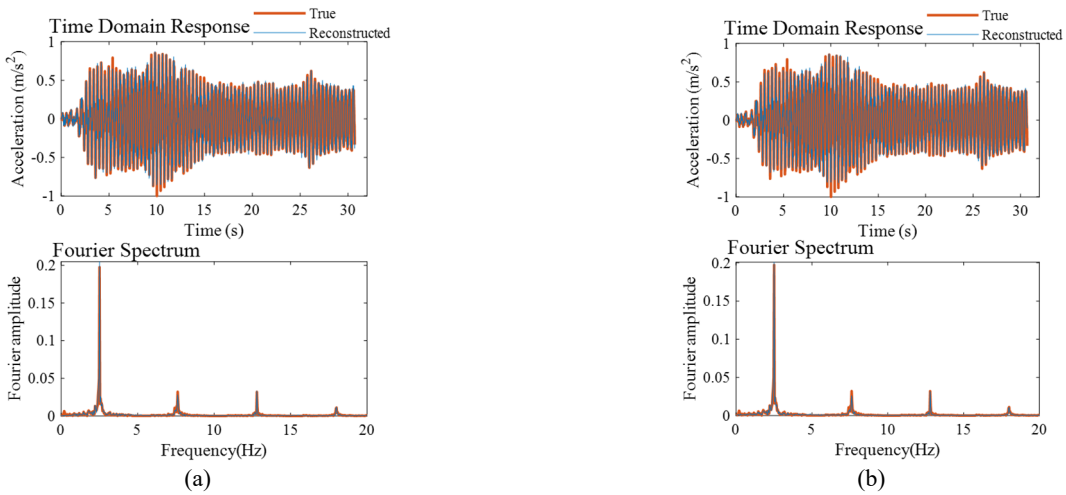

Fig. 16 Comparison of true and reconstructed responses under earthquake excitations: (a) UAGAN; and (b) CNN

Table 2 Comparison of identified modal parameters from real and reconstructed earthquake responses

Mode	f_{real} (Hz)	f_{re} (Hz)	$error_f$ (%)
1	2.54	2.54	0.00
2	7.62	7.62	0.00
3	12.79	12.79	0.00
4	17.97	17.97	0.00
5	22.75	22.75	0.00
6	26.86	26.86	0.00
COMAC = 99.96%			

*f: frequency; $error_f = \frac{f_{re}-f_{real}}{f_{real}}$

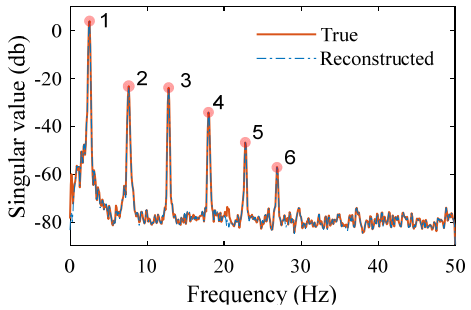

Fig. 17 Comparison of the FDD spectra of reconstructed and true responses under earthquake

representative features of data and accurately reconstruct the responses under structural condition changes with few-shot learning.

5. Conclusions

In this paper, a novel network UAGAN is proposed to learn the mapping between responses and reconstruct the structural response after structural states change. The theoretical developments of the imbedded advanced U-shaped dense block and self-attention module are explained in detail. Both the numerical and experimental studies demonstrate that the proposed UAGAN is capable of extracting universal and representative features and establishing robust mappings between responses by using a small number of sample datasets. The capability of UAGAN is verified by the accuracy of reconstructed responses in time and frequency domains and the consistent modal parameters that are identified from the reconstructed and corresponding actual responses. The remarkable performance of UAGAN indicates that the proposed approach is applicable and accurate for real applications. Further studies may be conducted to investigate the performance of the proposed method for response reconstruction of nonlinear systems.

Acknowledgments

The support from the National Natural Science Foundation of China project No. 52178279 and Guangzhou Basic and Applied Basic Research Foundation project, is greatly appreciated.

References

Bao, Y. and Li, H. (2021), "Machine learning paradigm for structural health monitoring", *Struct. Health Monitor.*, **20**(4), 1353-1372. https://doi.org/10.1177/1475921720972416

Bao, Y., Li, H., Sun, X., Yu, Y. and Ou, J. (2013), "Compressive sampling–based data loss recovery for wireless sensor networks used in civil structural health monitoring", *Struct. Health Monitor.*, **12**(1), 78-95. https://doi.org/10.1177/1475921712462936

Bao, J., Chen, D., Wen, F., Li, H. and Hua, G. (2017), "CVAE-GAN: fine-grained image generation through asymmetric training", *Proceedings of 2017 IEEE International Conference on Computer Vision* (*ICCV*), Venice, Italy, October.

Cross, E.J., Koo, K.Y., Brownjohn, J.M.W. and Worden, K. (2013), "Long-term monitoring and data analysis of the Tamar Bridge", *Mech. Syst. Signal Process.*, **35**(1-2), 16-34. https://doi.org/10.1016/j.ymssp.2012.08.026

Fan, G., Li, J. and Hao, H. (2019), "Lost data recovery for structural health monitoring based on convolutional neural networks", *Struct. Control Health Monitor.*, **26**(10), e2433. https://doi.org/10.1002/stc.2433

Fan, G., Li, J. and Hao, H. (2020), "Vibration signal denoising for structural health monitoring by residual convolutional neural networks", *Measurement*, **157**, p. 107651. https://doi.org/10.1016/j.measurement.2020.107651

Fan, G., Li, J. and Hao, H. (2021a), "Dynamic response reconstruction for structural health monitoring using densely connected convolutional networks", *Struct. Health Monitor.*, **20**(4), 1373-1391. https://doi.org/10.1177/1475921720916881

Fan, G., Li, J., Hao, H. and Xin, Y. (2021b), "Data driven structural dynamic response reconstruction using segment based generative adversarial networks", *Eng. Struct.*, **234**, p. 111970. https://doi.org/10.1016/j.engstruct.2021.111970

Goodfellow, I., Pouget-Abadie, J., Mirza, M., Xu, B., Warde-Farley, D., Ozair, S., Courville, A. and Bengio, Y. (2020), "Generative adversarial networks", *Commun. ACM*, **63**(11), 139-144. https://doi.org/10.1145/3422622

He, J., Zhou, Y., Guan, X., Zhang, W., Zhang, W. and Liu, Y. (2016), "Time domain strain/stress reconstruction based on empirical mode decomposition: numerical study and experimental validation", *Sensors*, **16**(8), 22. https://doi.org/10.3390/s16081290

Huang, Y., Beck, J.L., Wu, S. and Li, H. (2014), "Robust Bayesian compressive sensing for signals in structural health monitoring", *Comput.-Aided Civil Infrastr. Eng.*, **29**(3), 160-179. https://doi.org/10.1111/mice.12051

Jeong, S., Ferguson, M., Hou, R., Lynch, J.P., Sohn, H. and Law, K.H. (2019), "Sensor data reconstruction using bidirectional recurrent neural network with application to bridge monitoring", *Adv. Eng. Inform.*, **42**, p. 100991. https://doi.org/10.1016/j.aei.2019.100991

Jiang, K., Han, Q., Du, X. and Ni, P. (2021a), "Structural dynamic response reconstruction and virtual sensing using a sequence to sequence modeling with attention mechanism", *Automat. Constr.*, **131**, p. 103895. https://doi.org/10.1016/j.autcon.2021.103895

Jiang, H., Wan, C., Yang, K., Ding, Y. and Xue, S. (2021b), "Continuous missing data imputation with incomplete dataset by generative adversarial networks–based unsupervised learning for long-term bridge health monitoring", *Struct. Health Monitor.*, **21**(3), 1093-1109.

https://doi.org/10.1177/14759217211021942
Kalman, R.E. (1960), "A new approach to linear filtering and prediction problems", *J. Basic Eng.*, **82**(1), 35-45. https://doi.org/10.1115/1.3662552
Klikowicz, P., Salamak, M. and Poprawa, G. (2016), "Structural health monitoring of urban structures", In: *World Multidisciplinary Civil Engineering – Architecture – Urban Planning Symposium* (*WMCAUS*), Prague, Czech, August.
Kullaa, J. (2013), "Detection, identification, and quantification of sensor fault in a sensor network", *Mech. Syst. Signal Process.*, **40**(1), 208-221. https://doi.org/10.1016/j.ymssp.2013.05.007
Law, S.S., Li, J. and Ding, Y. (2011), "Structural response reconstruction with transmissibility concept in frequency domain", *Mech. Syst. Signal Process.*, **25**(3), 952-968. https://doi.org/10.1016/j.ymssp.2010.10.001
Lei, X., Sun, L. and Xia, Y. (2021), "Lost data reconstruction for structural health monitoring using deep convolutional generative adversarial networks", *Struct. Health Monitor.*, **20**(4), 2069-2087. https://doi.org/10.1177/1475921720959226
Li, J. and Hao, H. (2014), "Substructure damage identification based on wavelet-domain response reconstruction", *Eng. Struct.*, **13**(4), 389-405. https://doi.org/10.1177/1475921714532991
Li, J., Law, S.S. and Ding, Y. (2012), "Substructure damage identification based on response reconstruction in frequency domain and model updating", *Eng. Struct.*, **41**, 270-284. https://doi.org/10.1016/j.engstruct.2012.03.035
Li, J., Law, S.S. and Ding, Y. (2013), "Damage detection of a substructure based on response reconstruction in frequency domain", *Key Eng. Mater.*, **569**, 823-830. https://doi.org/10.4028/www.scientific.net/KEM.569-570.823
Li, J., Hao, H., Fan, G., Ni, P., Wang, X., Wu, C., Lee, J.M. and Jung, K.H. (2017), "Numerical and experimental verifications on damping identification with model updating and vibration monitoring data", *Smart Struct. Syst., Int. J.*, **20**(2), 127-137. https://doi.org/10.12989/sss.2017.20.2.127
Li, Y., Ni, P., Sun, L. and Zhu, W. (2022), "A convolutional neural network-based full-field response reconstruction framework with multitype inputs and outputs", *Struct. Control Health Monitor.*, p. e2961. https://doi.org/10.1002/stc.2961
Lin, Y.Z., Nie, Z.H. and Ma, H.W. (2017), "Structural damage detection with automatic feature-extraction through deep learning", *Comput.-Aided Civil Infrastr. Eng.*, **32**(12), 1025-1046. https://doi.org/10.1111/mice.12313
Lin, Z., Li, M., Zheng, Z., Cheng, Y. and Yuan, C. (2020), "Self-attention convlstm for spatiotemporal prediction", *Proceedings of the AAAI Conference on Artificial Intelligence*, New York, NY, USA, February.
Luong, M.T., Pham, H. and Manning, C.D. (2015), "Effective approaches to attention-based neural machine translation", arXiv preprint arXiv:1508.04025. https://doi.org/10.48550/arXiv.1508.04025
Nagarajaiah, S. and Erazo, K. (2016), "Structural monitoring and identification of civil infrastructure in the United States", *Struct. Monitor. Maint., Int. J.*, **3**(1), 51-69. https://doi.org/10.12989/smm.2016.3.1.051
Ni, P., Li, J., Hao, H. and Xia, Y. (2018), "Stochastic dynamic analysis of marine risers considering Gaussian system uncertainties", *J. Sound Vib.*, **416**, 224-243. https://doi.org/10.1016/j.jsv.2017.11.049
Ni, P., Li, J., Hao, H., Xia, Y. and Du, X. (2019a), "Stochastic dynamic analysis of marine risers considering fluid-structure interaction and system uncertainties", *Eng. Struct.*, **198**, 14. https://doi.org/10.1016/j.engstruct.2019.109507
Ni, P., Xia, Y., Li, J., Hao, H., Bi, K. and Zuo, H. (2019b), "Multi-scale stochastic dynamic response analysis of offshore risers with lognormal uncertainties", *Ocean Eng.*, **189**, p. 106333. https://doi.org/10.1016/j.oceaneng.2019.106333
Niu, Y., Fritzen, C.P., Jung, H., Buethe, I., Ni, Y.Q. and Wang, Y.W. (2015), "Online simultaneous reconstruction of wind load and structural responses—Theory and application to Canton Tower", *Comput.-Aided Civil Infrastr. Eng.*, **30**(8), 666-681. https://doi.org/10.1111/mice.12134
Oh, B.K., Glisic, B., Kim, Y. and Park, H.S. (2020), "Convolutional neural network-based data recovery method for structural health monitoring", *Struct. Health Monitor.*, **19**(6), 1821-1838. https://doi.org/10.1177/1475921719897571
Petersen, Ø.W., Øiseth, O., Nord, T.S. and Lourens, E. (2018), "Estimation of the full-field dynamic response of a floating bridge using Kalman-type filtering algorithms", *Mech. Syst. Signal Process.*, **107**, 12-28. https://doi.org/10.1016/j.ymssp.2018.01.022
Ronneberger, O., Fischer, P. and Brox, T. (2015), "U-net: Convolutional networks for biomedical image segmentation", *International Conference on Medical Image Computing and Computer-Assisted Intervention*, November.
Sun, L., Shang, Z., Xia, Y., Bhowmick, S. and Nagarajaiah, S. (2020), "Review of bridge structural health monitoring aided by big data and artificial intelligence: From condition assessment to damage detection", *J. Struct. Eng.*, **146**(5), 04020073. https://doi.org/10.1061/(asce)st.1943-541x.0002535
Thadikemalla, V.S.G. and Gandhi, A.S. (2018), "A data loss recovery technique using compressive sensing for structural health monitoring applications", *KSCE J. Civil Eng.*, **22**(12), 5084-5093. https://doi.org/10.1007/s12205-017-2070-z
Vaswani, A., Shazeer, N., Parmar, N., Uszkoreit, J., Jones, L., Gomez, A.N., Kaiser, Ł. and Polosukhin, I. (2017), "Attention is all you need", *Proceedings of the 31st International Conference on Neural Information Processing Systems*, Long Beach, CA, USA, December.
Wan, Z., Wang, T., Huang, Q. and Li, L. (2014), "Structural response reconstruction for non-proportionally damped systems in the presence of closely spaced modes", *J. Vibroeng.*, **16**(8), 3740-3758. https://www.extrica.com/article/15202
Xu, T., Zhang, P., Huang, Q., Zhang, H., Gan, Z., Huang, X. and He, X. (2018), "Attngan: Fine-grained text to image generation with attentional generative adversarial networks", *Proceedings of the 2018 IEEE/CVF Conference on Computer Vision and Pattern Recognition*, Salt Lake City, UT, USA, June.
Yi, T.H., Li, H.N. and Gu, M. (2013), "Recent research and applications of GPS-based monitoring technology for high-rise structures", *Struct. Control Health Monitor.*, **20**(5), 649-670. https://doi.org/10.1002/stc.1501
Zhang, Y. and Lei, Y. (2021), "Data anomaly detection of bridge structures using convolutional neural network based on structural vibration signals", *Symmetry*, **13**(7), p. 1186. https://doi.org/10.3390/sym13071186
Zhang, X.H. and Wu, Z.B. (2019), "Dual-type structural response reconstruction based on moving-window Kalman filter with unknown measurement noise", *J. Aerosp. Eng.*, **32**(4), 14. https://doi.org/10.1061/(asce)as.1943-5525.0001016
Zhang, C.D. and Xu, Y.L. (2016), "Structural damage identification via multi-type sensors and response reconstruction", *Struct. Health Monitor.*, **15**(6), 715-729. https://doi.org/10.1177/1475921716659787
Zhang, L., Ji, Y., Lin, X. and Liu, C. (2017), "Style transfer for anime sketches with enhanced residual u-net and auxiliary classifier gan", In: *2017 4th IAPR Asian Conference on Pattern Recognition* (*ACPR*), Nanjing, China, November.
Zhang, X.H., Zhu, Z., Yuan, G.K. and Zhu, S. (2021), "Adaptive Mode Selection Integrating Kalman Filter for Dynamic Response Reconstruction", *J. Sound Vib.*, **515**, 18. https://doi.org/10.1016/j.jsv.2021.116497
Zhou, H., Zhang, S., Peng, J., Zhang, S., Li, J., Xiong, H. and

Zhang, W. (2021), "Informer: Beyond efficient transformer for long sequence time-series forecasting", *Proceedings of the AAAI Conference on Artificial Intelligence*, Vol. 35, No. 12, February.

Zhu, S., Zhang, X.H., Xu, Y.L. and Zhan, S. (2013), "Multi-type sensor placement for multi-scale response reconstruction", *Adv. Struct. Eng.*, **16**(10), 1779-1797. https://doi.org/10.1260/1369-4332.16.10.1779